Image Cover Sheet

CLASSIFICATION	SYSTEM NUMBER
UNCLASSIFIED	510310

TITLE

J-RESISTANCE CURVE OF HY100

System Number:

Patron Number:

Requester:

Notes: Paper #5 contained in Parent Sysnum #510305

DSIS Use only:

Deliver to: DK

#510310 (5)

J-Resistance Curve of HY100

by Dr. B. Faucher and Dr. K. Karis Allen

Metals Technology Laboratories, CANMET, Energy Mines & Resources Canada, 568 Booth, Ottawa, K1A 0G1
and
Defence Research Establishment Atlantic, Dockyard Laboratory FMO Halifax, Halifax, Nova Scotia, B3K 2X0

ABSTRACT

A precise knowledge of toughness of materials is needed to evaluate the fitness-for-purpose of structures with defects. For brittle materials as steels at low temperatures, the toughness is measured with the stress intensity factor, K. Steels at high temperature are tough and their toughness is then measured either with the CTOD (Crack tip opening displacement) or the J-integral. These quantities are related as:

$$J = K^2/E = \sigma_y \ (CTOD)$$

where E and σ_y are material's Young's modulus and yield strength, respectively. Increasing resistance of material to crack advance during tearing is taken into account by the J-resistance curve. It is a graph of J as a function of crack extension. J is obtained from experimental load-deformation curve, and crack extension from different techniques to monitor crack length during the test; the most common one, standardized by ASTM, is the unloading technique which requires to stop the test for a short period of time to measure the compliance of the specimen at regular intervals. This technique is delicate of application, time consuming and, of course, not applicable to impact testing.

An alternative method to obtain the crack length is by comparing the experimental load-displacement curve to a reference curve, the "key-curve", obtained for a specimen with no crack extension. In this method, the crack extension is obtained by numerical calculations from the difference between the two load-displacement curves. The key-curve may be either measured from experiment with sub-size or blunt-notch specimens, calculated from the tensile properties of the material, or obtained directly from the test with the growing crack. The aim of these approaches is to derive a simplified method to measure experimentally the J-resistance curve, and contribute to increasing the use of J_{Ic} as a convenient toughness parameter

Preliminary results on the effectiveness of the key-curve will be presented by comparing key-curves of HY100, calculated with the standardized unloading compliance method and the key-curve approach.

J-RESISTANCE CURVE OF HY 100

B. Faucher[1] and K. KarisAllen[2]

[1]Metals Technology Laboratories, CANMET
Energy Mines & Resources Canada, 568 Booth, Ottawa, K1A 0G1
and
[2]Defence Research Establishment Atlantic, Dockyard Laboratory
FMO Halifax, Halifax, Nova Scotia, B3K 2X0

Presented at the Canadian Forces CRAD meeting on "Naval Applications of Materials Technology", Halifax, April 1993.

The J-resistance curve of HY 100 has been obtained for several specimen geometries with the standardized unloading compliance technique and the key-curve method.

EXPERIMENTAL

The specimens were all taken from a one inch thick armour plate of HY100 MIL-S-16216J, austenitized at 905°C for 70 minutes, water-quenched and then tempered at 660°C for 70 minutes. A typical microstructure is shown in Fig.1. The average yield and tensile strength measured with three standard tensile specimens are 818 and 937 MPa, respectively. Compact C(T), and three-point-bend SE(B), specimens were prepared according to ASTM E-813 Standard for J_{Ic} Testing. The thickness was 25 mm, large enough to ensure valid J_{Ic} values. Three different values of crack length, a/W = 0.25, 0.5, and 0.75, were used for SE(B) and the two larger values for C(T) specimens. Specimens were made with 20% side-grooves (SG) and without side-grooves (Fig.2). The standardized (E813) unloading technique was used to obtain J-resistance curves. Experimental key-curves were determined using specimens without fatigue precracks.

The tests were carried out in a servo-hydraulic universal testing machine at a displacement rate of 0.01 mm/s. Test control and data acquisition were performed with an Instron 8500 controller, using dedicated software for machine control and data acquisition developed and implemented on an IBM compatible PC. A typical graph of the load as a function of load-line displacement is shown with the unloading cycles in Fig.3. The extraneous displacement for the bend specimens was fitted with a fourth degree polynomial and subtracted from the measured overall load-line displacement. After testing, the specimens were heat-tinted at 375°C for 15 minutes, cooled at liquid nitrogen temperature, and broken open to measure the initial and final crack lengths. Typical fracture surfaces show the fatigue precrack and the crack advance.

UNLOADING COMPLIANCE

Typical J-resistance curves are shown for the various geometries in Figs.4 and 5. Side-grooves promote a state of plane strain , i.e. increase the out-of-plane constraint. The effect is obvious on the tearing resistance (the slope of the J-resistance curve), which is much smaller for SG specimens. The critical value of J, J_{Ic}, defined by the intersection of the J-resistance curve with the 0.2 mm offset blunting line, is not affected significantly neither by the crack length, nor by the side-grooves, except for bend specimens with the shallowest initial crack lengths which have also the highest values of the tearing resistance. This effect may be quantified by an in-plane constraint parameter such as the T-stress (Fig.6). The results show that the toughness may be significantly larger for negative values of the T-stress, that is for shallow cracks loaded in bending. Tension loading, which is characterized by large negative T values, could also exhibit high toughness.

KEY-CURVE

The key-curve method is based on the assumption that the load, P, can be expressed as separable multiplicative functions of crack length, a, and plastic component of load line displacement, Δ_p:

$$P = G\left(\frac{a}{W}\right) H\left(\frac{\Delta_p}{W}\right)$$

where W is the specimen width. For deeply cracked bend type specimens in the fully plastic range, the function G(a/W) is proportional to b^2, the square of the remaining ligament (b=W-a). The load varies also with the specimen net section thickness, B_N, and the material flow stress, σ_f, the average between yield and tensile strengths, so that we may write:

$$H\left(\frac{\Delta_{pl}}{W}\right) = \frac{P}{G(a/W)} = \frac{4PW}{B_N b^2 \sigma_f}$$

Defining the normalized load as:

$$P_N = \frac{4PW}{B_N b_o^2 \sigma_f}$$

the crack length is obtained as:

$$\Delta a = b_o \left(1 - \sqrt{H / P_N}\right).$$

For compact, C(T), specimens:

$$H\left(\frac{\Delta_{pl}}{W}\right) = \frac{P}{G(a/W)} = \frac{4PW}{B_N b^2 \sigma_f \exp(0.522 b/W)}$$

and we define the normalized load as:

$$P_N = \frac{4PW}{B_N b_o^2 \sigma_f \exp(0.522 b_o/W)}.$$

Hence, for small increments of crack extension:

$$\Delta a \simeq \frac{b_o\left(1-\sqrt{H/P_N}\right)}{1+0.261 b_o\sqrt{H/P_N}/W}$$

The key curve (the function H) can be determined from the crack length obtained from the unloading compliance. It is compared to the load normalized with the initial crack length in Fig.7. Alternatively, crack extension is easily determined, if the key-curve is known. An "experimental" key-curve can be obtained with specimens with blunt notches for which crack extension starts at larger values of deformation than for specimens with sharp cracks. It is also possible to use a functional relationship for the key curve (or "calibration" curve). Two possibilities are the power law:

$$H = H_o\ (\Delta_p/W)^n$$

and the so-called "LMN" function:

$$H = \frac{L + M\Delta_{pl}/W}{N + \Delta_{pl}/W}\ \Delta_{pl}/W$$

In this work, the parameters H_o and n, and L,M, and N have been obtained from the last data point (where the crack length is known) and by fitting the key curve to the normalized experimental curve in the largest possible region just before maximum load. The calibration curves are compared with the normalized experimental curves for each of the methods in Figs.8, 10, and 12, and the resulting J-resistance curves are compared to the unloading compliance curve for one specimen in Figs. 9, 11, and 13. The calibration curves for all bend specimens are also shown in Fig.14 in terms of the crack-mouth-opening rather than load-line displacement.

CONCLUSIONS

The critical value of J is not affected significantly by the out-of-plane constraint (side-grooves); it changes with the in-plane constraint, i.e., it increases at large negative values of the T-stress. The tearing resistance (slope of the J-resistance curve) is affected significantly by the out-of-plane constraint.

Key-curve methods give reasonable values of the J-resistance curve; values of J_{Ic} seem to be somewhat larger than the value obtained by the unloading compliance method which is the most conservative.

ACKNOWLEDGEMENTS

Helpful discussions with Dr. W.R. Tyson are gratefully acknowledged.

BIBLIOGRAPHY

Ernst, Hugo, Paris, P.C., Rossow, Mark, and Hutchinson, J.W., **"Analysis of Load-Displacement Relationships to Determine J-R Curve and Tearing Instability Material Properties"**, in *Fracture Mechanics, ASTM STP 677*, C.W. Smith Ed., American Society for Testing and Materials, 1979, pp.581-599.

Joyce, J.A., Ernst, Hugo, and Paris, P.C., **"Direct Evaluation of J-Resistance Curves from Load Displacement Records"**, in *Fracture Mechanics: Twelfth Conference, ASTM STP 700*, American Society for Testing and Materials, 1980, pp.222-236.

Ernst, H. A., Paris, P.C., Landes, J.D., **"Estimations on J-Integral and Tearing Modulus T from a Single Specimen Test Record"**, in *Fracture Mechanics: Thirteenth Conference, ASTM STP 743*, Richard Roberts, Ed., American Society for Testing and Materials, 1981, pp. 476-502.

Landes, J.D., Zhou. Z., Lee, K., and Herrera, R., **"Normalization Method for Developing J-R Curves with the LMN Function"**, J. of Testing and Evaluation, 19, 4, 1991, pp. 305-311.

"Constraint Effects in Fracture",ASTM STP 1171, E. M. Hackett, R.-H. Schawlbe, and R. H. Dodds, Eds., American Society for Testing and Materials, Philadelphia, 1993.

"Shallow Crack Fracture Mechanics Toughness Tests and Applications", TWI, Cambridge, UK, 1992, Proceedings of an international conference, in press.

FIGURE CAPTIONS

Figure 1: Typical microstructure of the HY100 steel.

Figure 2: Fracture surfaces of bend specimens showing machined notch, fatigue pre-cracking, and ductile tearing for six different geometries.

Figure 3: Load as a function of the load-line displacement with unloadings to measure the compliances.

Figure 4: J-resistance curves for C(T) specimens.

Figure 5: J-resistance curves for bend specimens.

Figure 6: Critical values of J as a function of the constraint. Side-grooved (SG) specimens represent a lower bound for toughness; only some J_Q from SG specimens qualifies as J_{Ic}.

Figure 7: Comparison of the key-curve obtained from the unloading compliances with the normalized load. The displacement is normalized by the specimen width.

Figure 8: Comparison of the experimental key-curve with the normalized load.

Figure 9: Comparison of the J-resistance curves obtained with the experimental key-curve and with the unloading compliance (dots).

Figure 10: Comparison of the power law key-curve with the normalized load.

Figure 11: Comparison of the J-resistance curves obtained with the power law key-curve and with the unloading compliance (dots).

Figure 12: Comparison of the "LMN" key-curve with the normalized load.

Figure 13: Comparison of the J-resistance curves obtained with the "LMN" key-curve and with the unloading compliance (dots).

Figure 14: Comparison of the H-values obtained with the various key-curve methods as a function of the plastic CMOD.

Figure 1

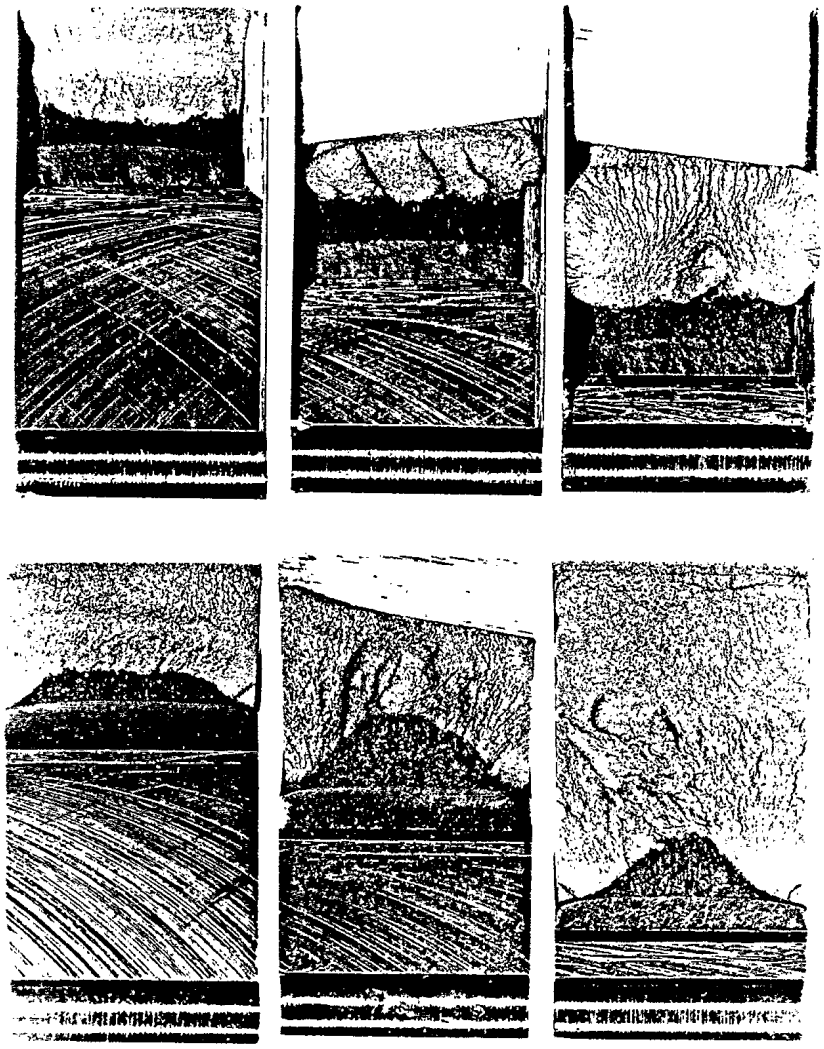

Figure 2

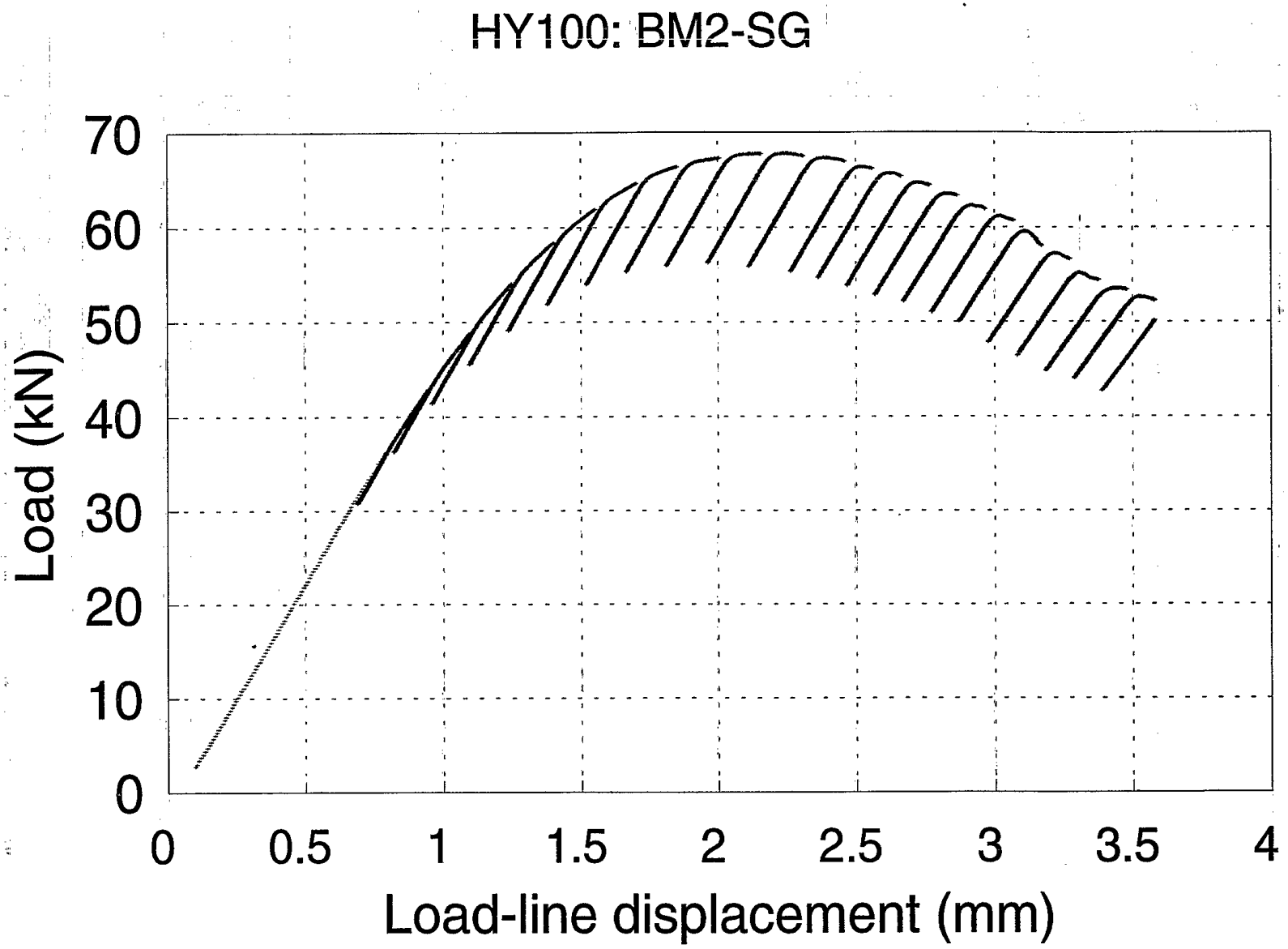
HY100: BM2-SG
Load (kN)
70
60
50
40
30
20
10
0
0
0.5
1
1.5
2
2.5
3
3.5
4
Load-line displacement (mm)

Figure 3

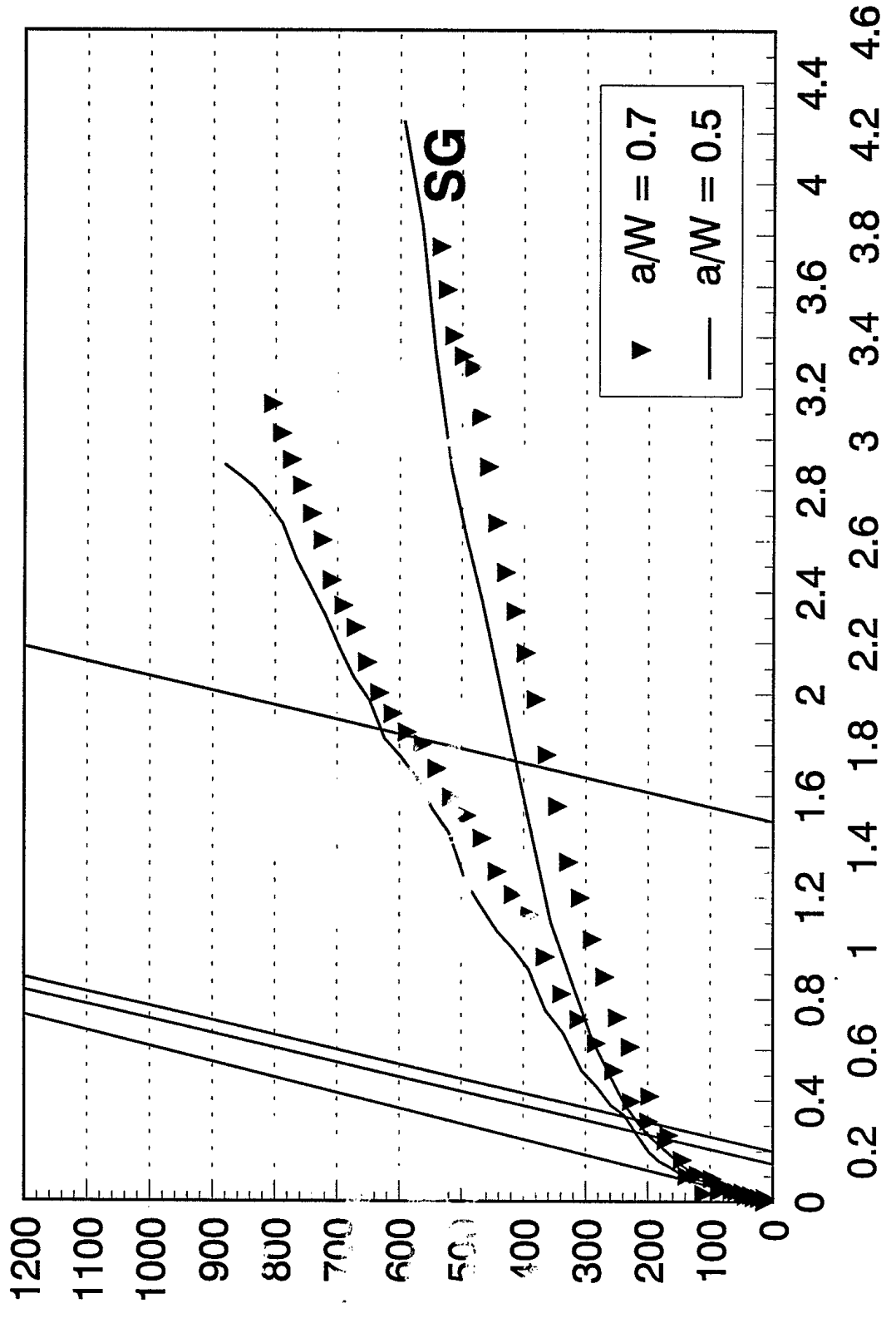
J (kJ/m²)
1200
1100
1000
900
800
700
600
500
400
300
200
100
0
0
0.2
0.4
0.6
0.8
1
1.2
1.4
1.6
1.8
2
2.2
2.4
2.6
2.8
3
3.2
3.4
3.6
3.8
4
4.2
4.4
4.6
Crack extension (mm)
SG
a/W = 0.7
a/W = 0.5

Figure 4

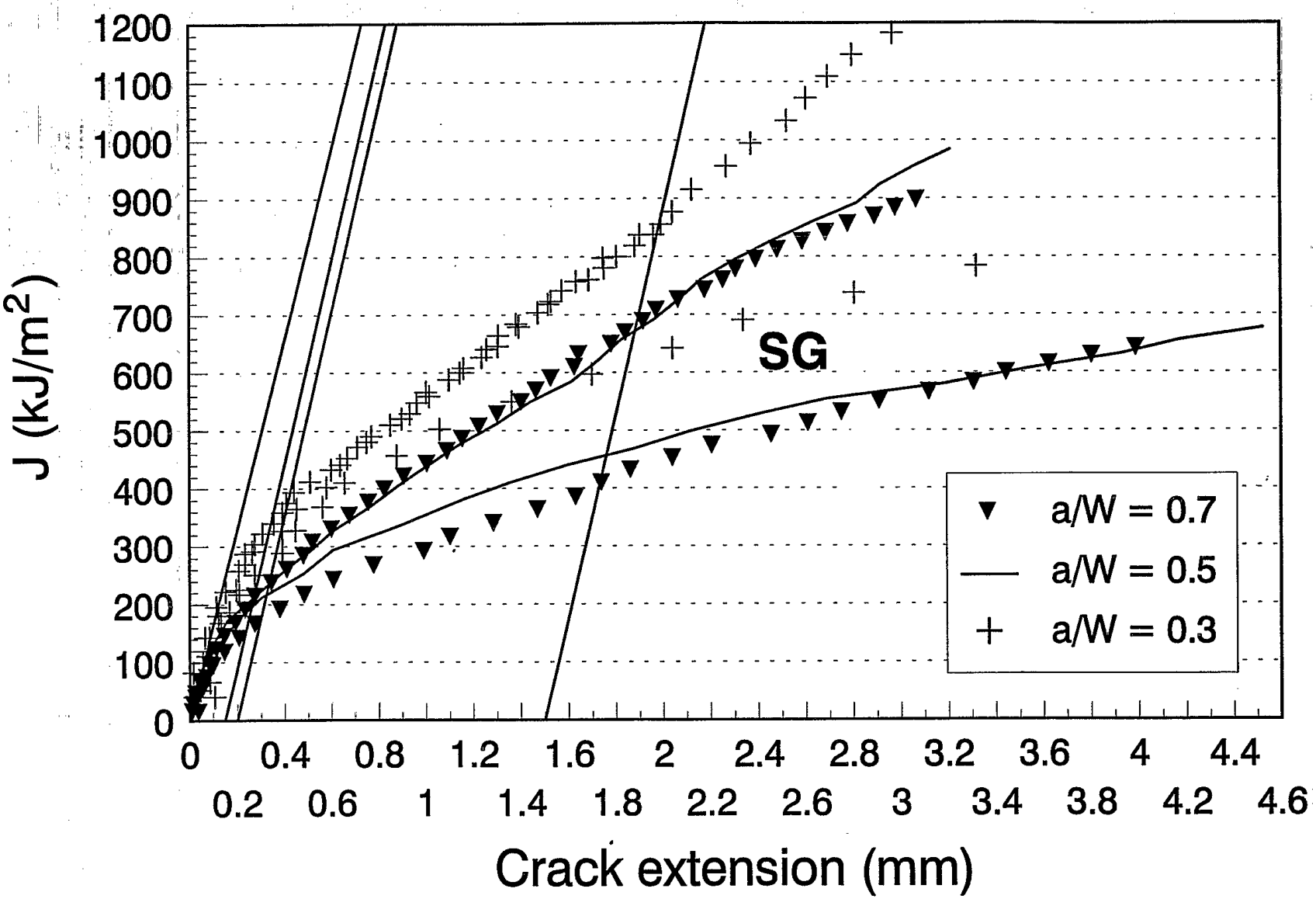
J (kJ/m2)
1200
1100
1000
900
800
700
600
500
400
300
200
100
0
0
0.2
0.4
0.6
0.8
1
1.2
1.4
1.6
1.8
2
2.2
2.4
2.6
2.8
3
3.2
3.4
3.6
3.8
4
4.2
4.4
4.6
Crack extension (mm)
SG
a/W = 0.7
a/W = 0.5
a/W = 0.3

Figure 5

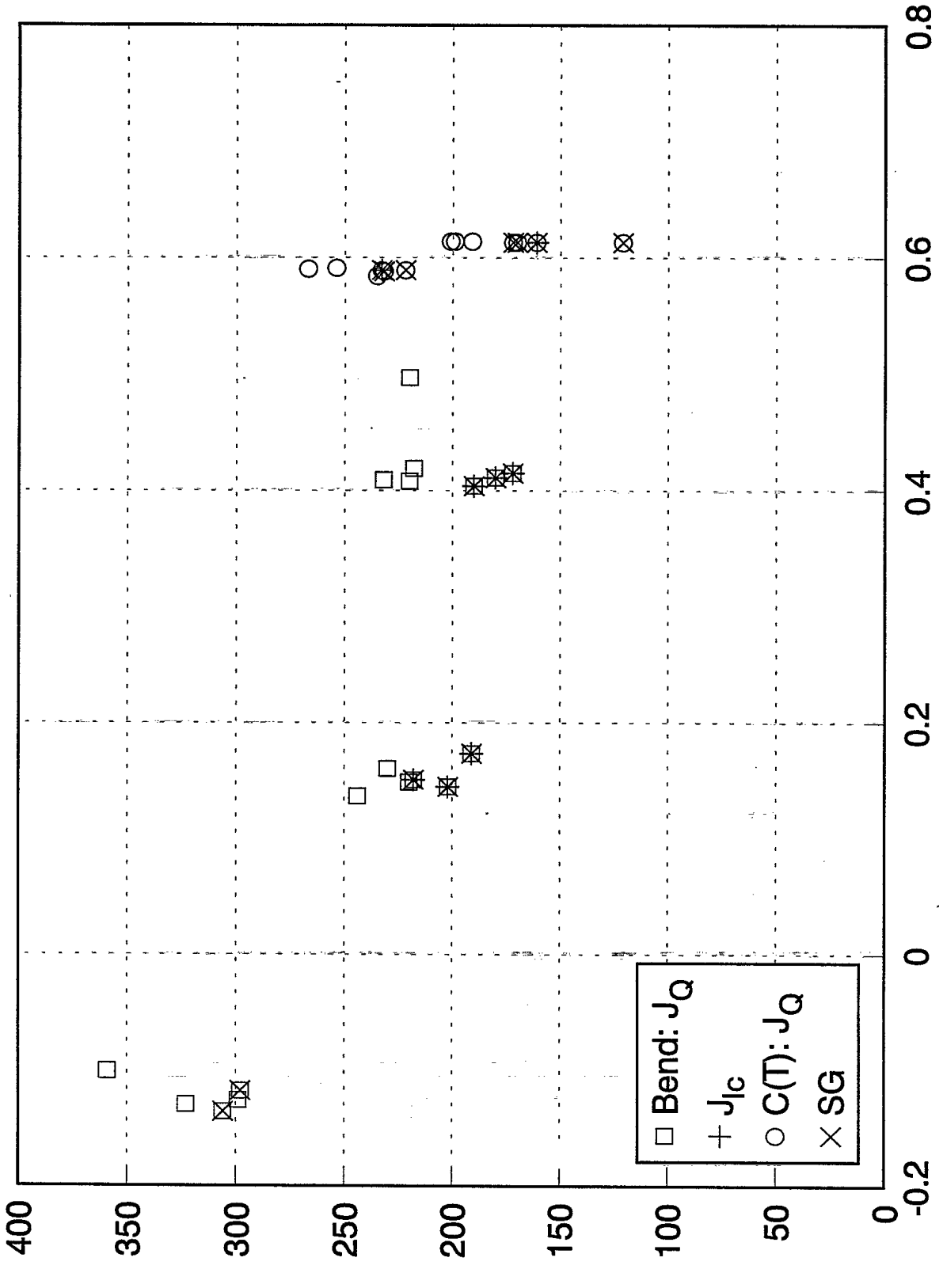
Critical values of J (kJ/m²)
T-stress
400
350
300
250
200
150
100
50
0
-0.2
0
0.2
0.4
0.6
0.8
□ Bend: J_Q
+ J_Ic
○ C(T): J_Q
× SG

Figure 6

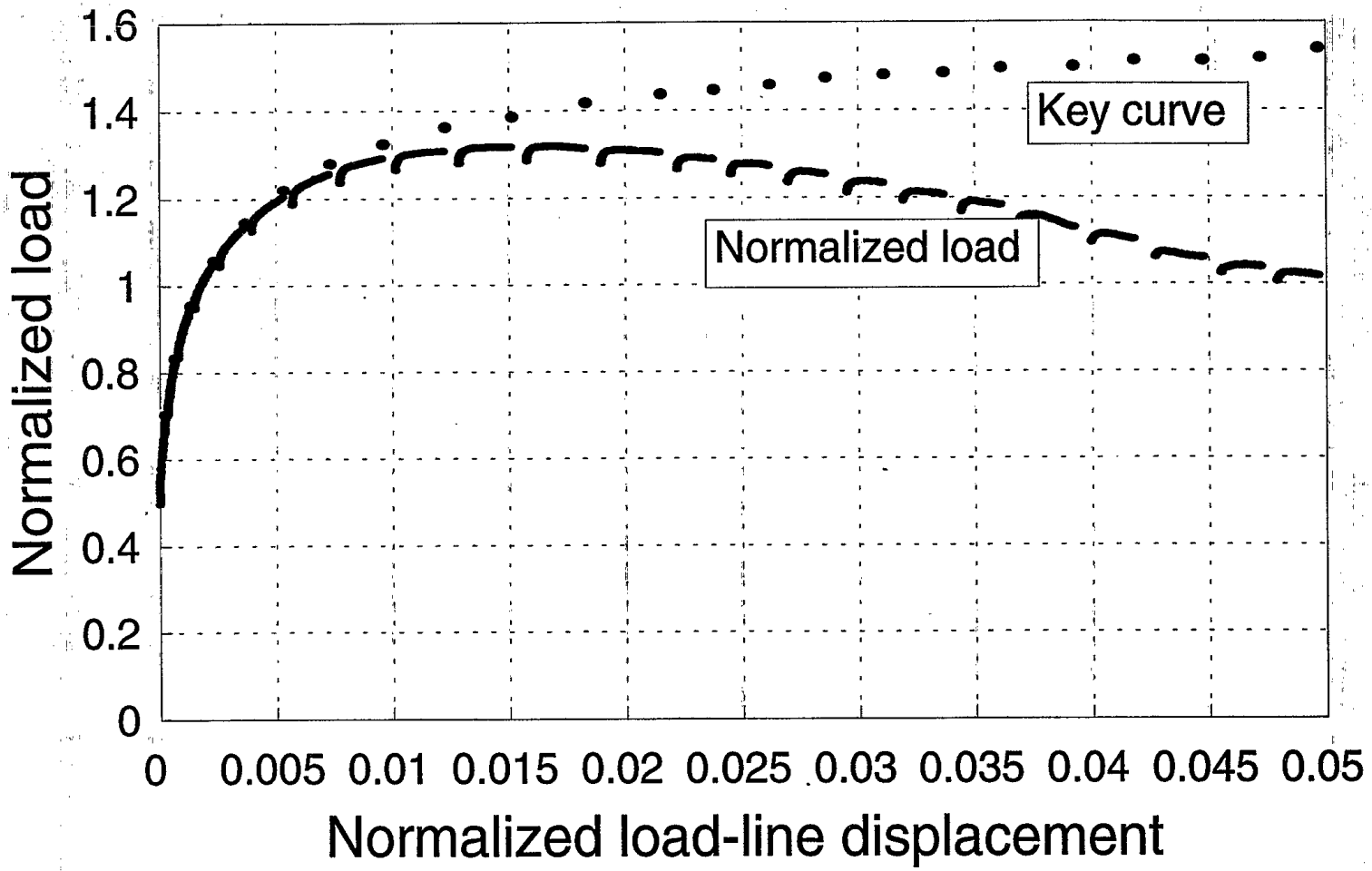
BM-2-SG Key curve: compliance
Key curve
Normalized load
Normalized load
Normalized load-line displacement
0
0.2
0.4
0.6
0.8
1
1.2
1.4
1.6
0
0.005
0.01
0.015
0.02
0.025
0.03
0.035
0.04
0.045
0.05

Figure 7

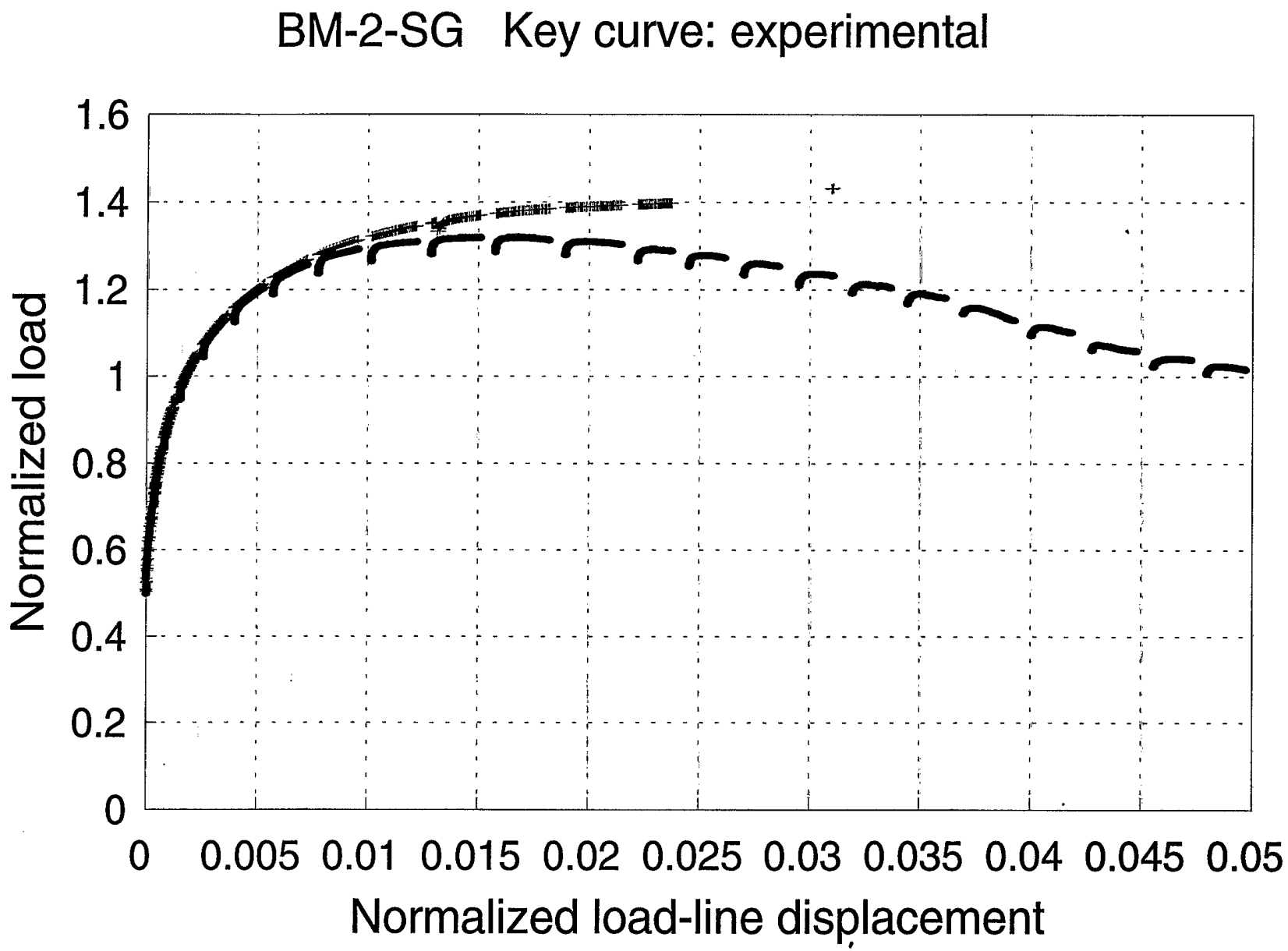
BM-2-SG Key curve: experimental
Normalized load
1.6
1.4
1.2
1
0.8
0.6
0.4
0.2
0
0 0.005 0.01 0.015 0.02 0.025 0.03 0.035 0.04 0.045 0.05
Normalized load-line displacement

Figure 8

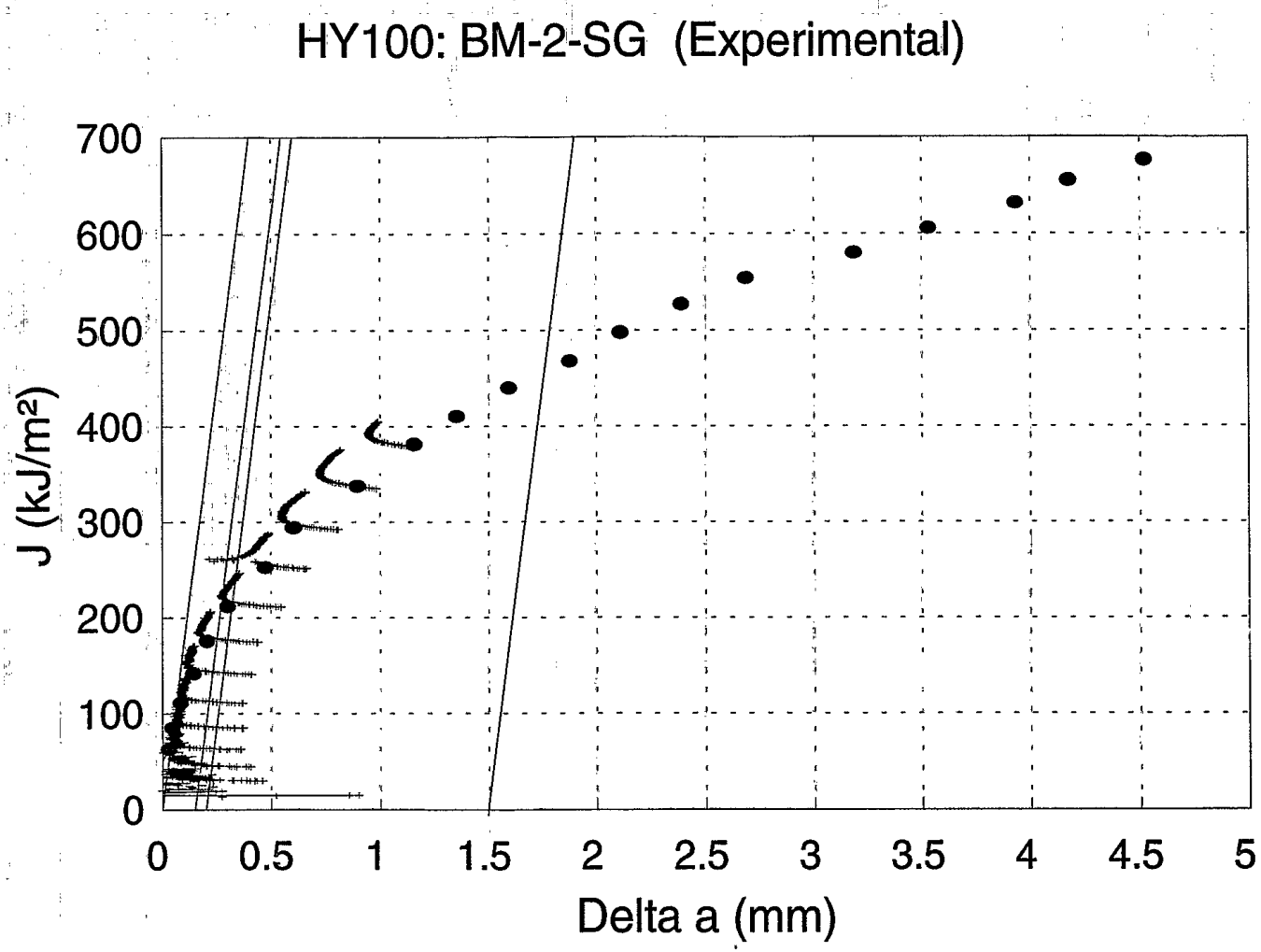
HY100: BM-2-SG (Experimental)
J (kJ/m²)
Delta a (mm)
0
100
200
300
400
500
600
700
0
0.5
1
1.5
2
2.5
3
3.5
4
4.5
5

Figure 9

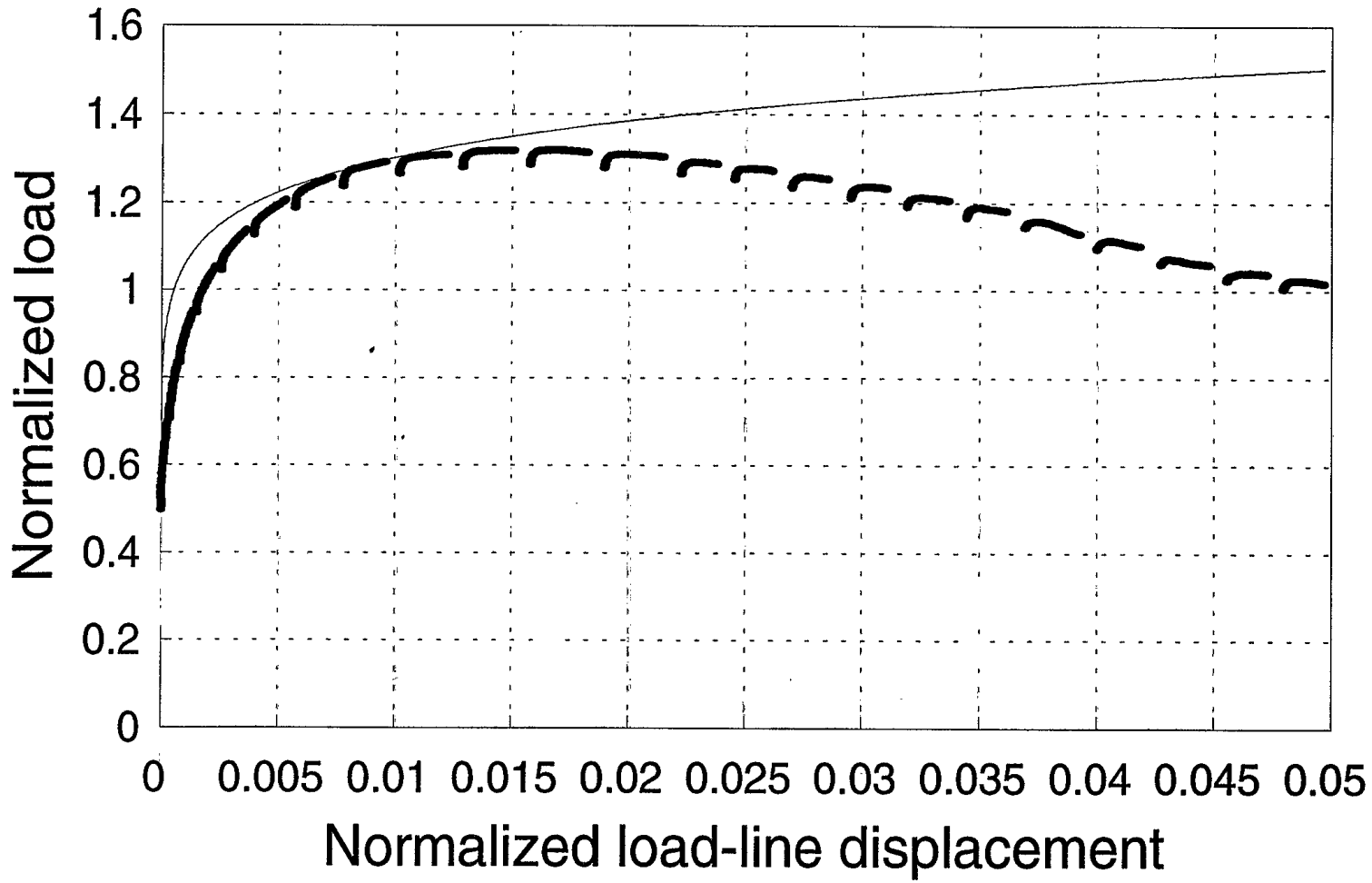
BM-2-SG Key curve: power law
Normalized load
1.6
1.4
1.2
1
0.8
0.6
0.4
0.2
0
0
0.005
0.01
0.015
0.02
0.025
0.03
0.035
0.04
0.045
0.05
Normalized load-line displacement

Figure 10

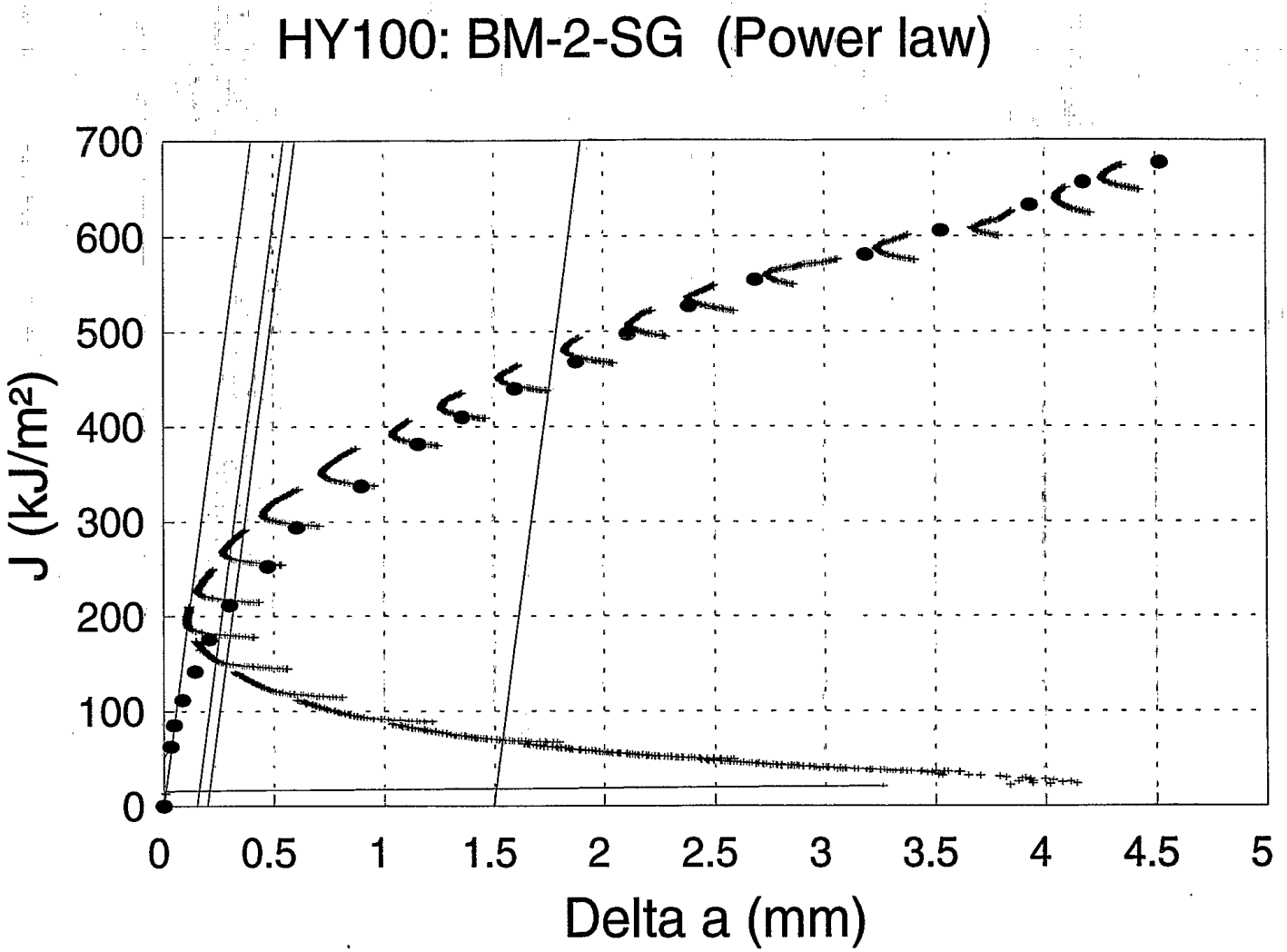
HY100: BM-2-SG (Power law)
J (kJ/m²)
700
600
500
400
300
200
100
0
0
0.5
1
1.5
2
2.5
3
3.5
4
4.5
5
Delta a (mm)

Figure 11

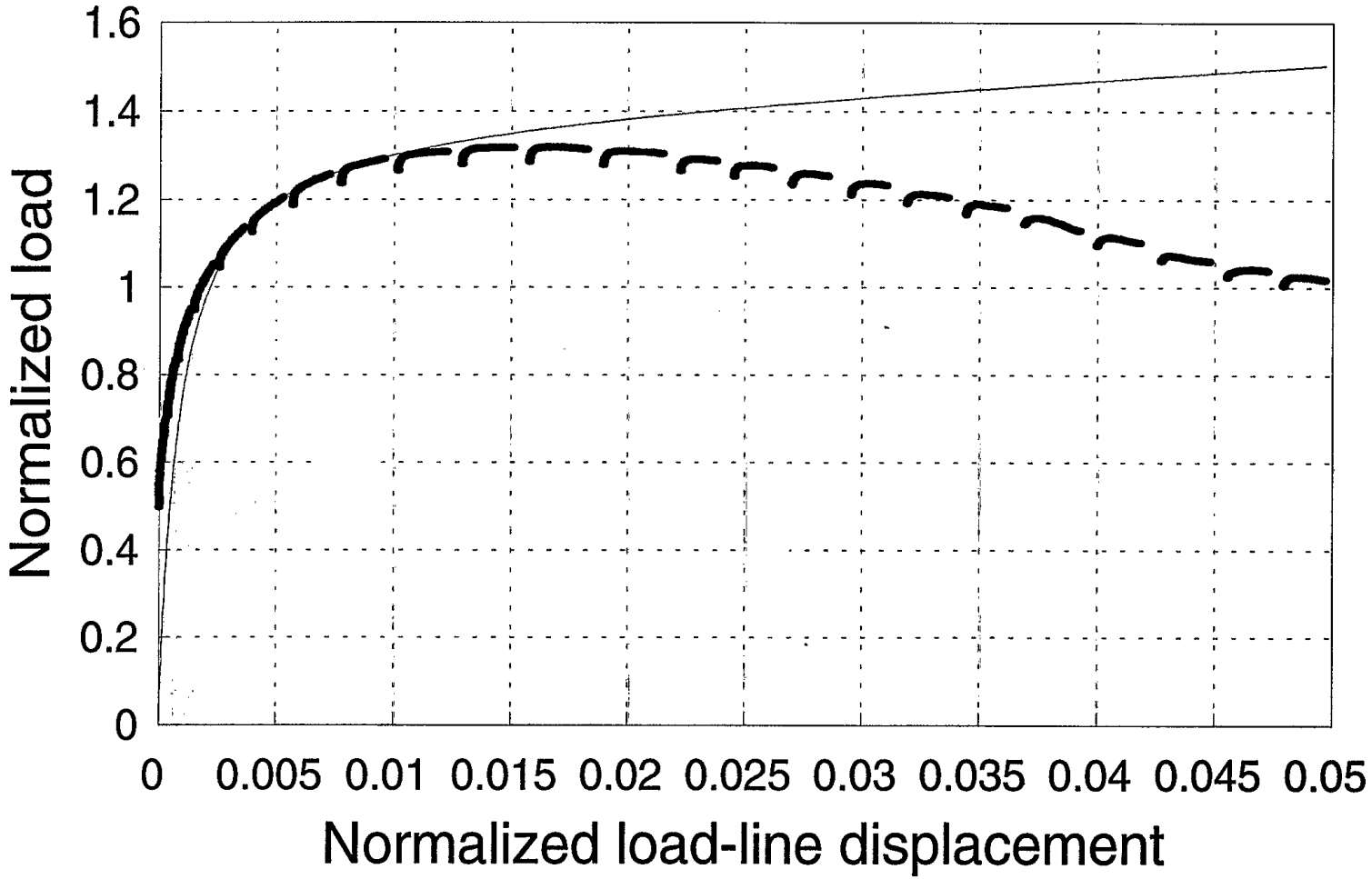
BM-2-SG Key curve: "LMN"
Normalized load
1.6
1.4
1.2
1
0.8
0.6
0.4
0.2
0
0 0.005 0.01 0.015 0.02 0.025 0.03 0.035 0.04 0.045 0.05
Normalized load-line displacement

Figure 12

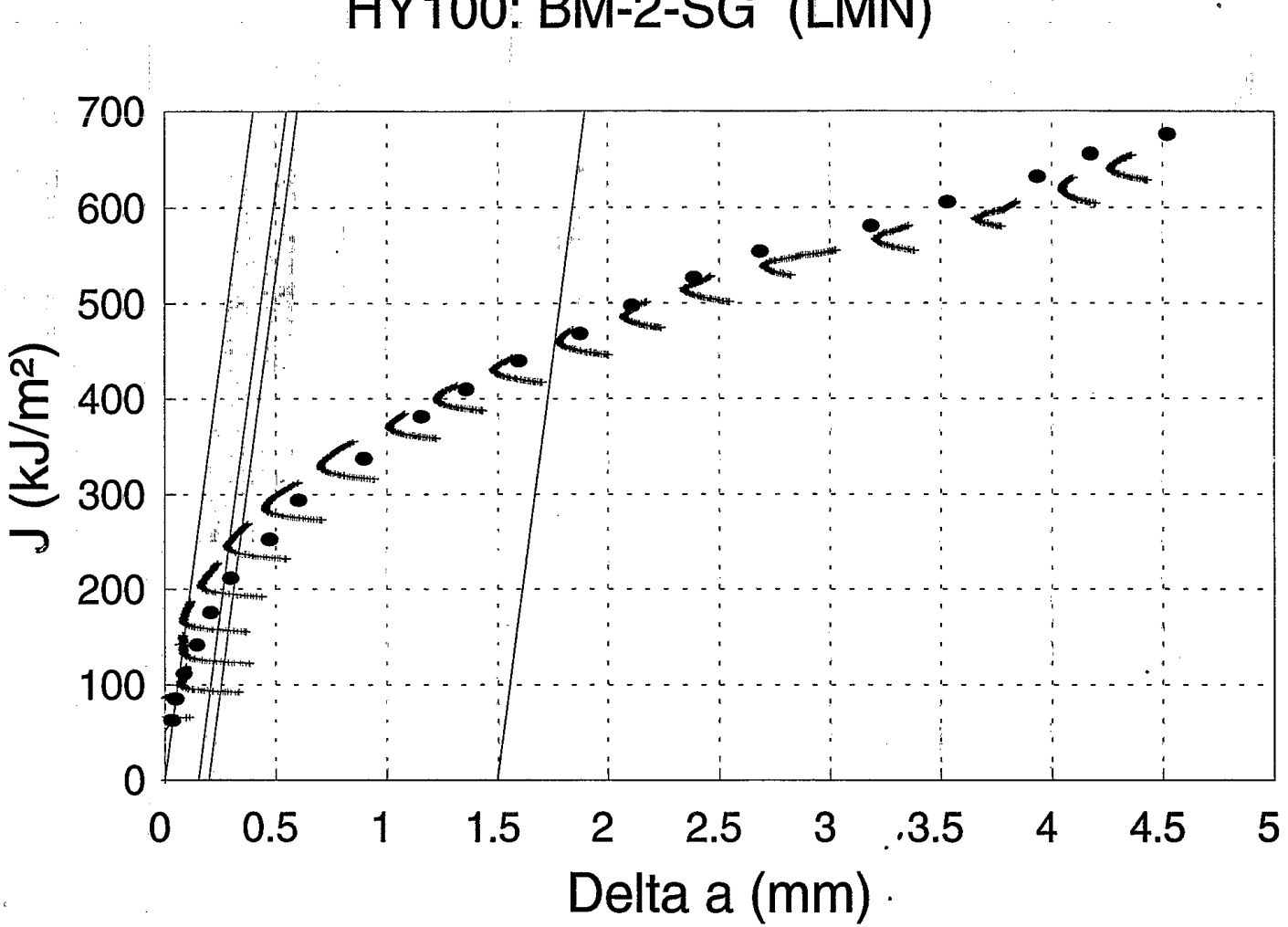
HY100: BM-2-SG (LMN)
J (kJ/m²)
700
600
500
400
300
200
100
0
0
0.5
1
1.5
2
2.5
3
3.5
4
4.5
5
Delta a (mm)

Figure 13

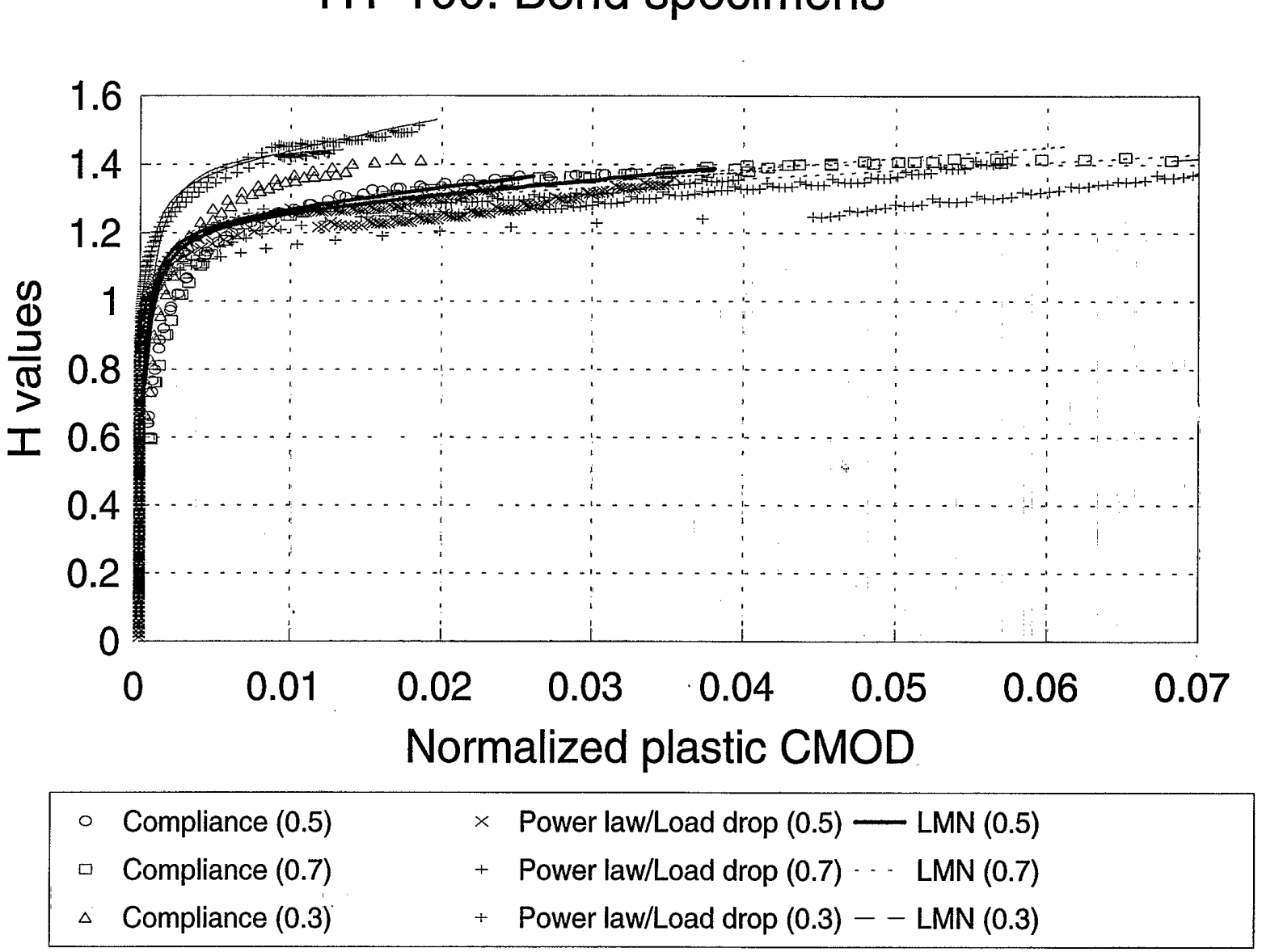
HY 100: Bend specimens
H values
1.6
1.4
1.2
1
0.8
0.6
0.4
0.2
0
0
0.01
0.02
0.03
0.04
0.05
0.06
0.07
Normalized plastic CMOD
Compliance (0.5)
Compliance (0.7)
Compliance (0.3)
Power law/Load drop (0.5)
Power law/Load drop (0.7)
Power law/Load drop (0.3)
LMN (0.5)
LMN (0.7)
LMN (0.3)

Figure 14